

Porous SiOC beads by freeze-drying polycarbosilane emulsions

The Faculty of Oregon State University has made this article openly available.
Please share how this access benefits you. Your story matters.

Citation	Hwang, Y., Riu, D. H., Kim, K. J., & Chang, C. H. (2014). Porous SiOC beads by freeze-drying polycarbosilane emulsions. <i>Materials Letters</i> , 131, 174-177. doi:10.1016/j.matlet.2014.05.194
DOI	10.1016/j.matlet.2014.05.194
Publisher	Elsevier
Version	Accepted Manuscript
Terms of Use	http://cdss.library.oregonstate.edu/sa-termsfuse

Porous SiOC beads by freeze-drying polycarbosilane emulsions

Yeon Hwang^{a*}, Doh-Hyung Riu^a, Ki-Joong Kim^b, Chih-Hung Chang^b

^a *Department of Materials Science & Engineering, Seoul National University of Science & Technology, Seoul 139-743, Republic of Korea*

^b *School of Chemical, Biological and Environmental Engineering, Oregon State University, Corvallis, Oregon 97331, USA*

* Corresponding author: Tel.: +82-2-970-6517; fax.: +82-2-973-6657.

E-mail address: yhwang@seoultech.ac.kr

ABSTRACT

Porous silicon oxycarbide (SiOC) beads were prepared by freeze-drying of water-in-oil (w/o) emulsion, containing water and polycarbosilane (PCS) dissolved *p*-xylene in the presence of sodium xylenesulfonate (SXS) as an emulsifier. The emulsion was frozen by being dropped onto a liquid N₂ bath, which resulted in 1~2 mm sized beads. After curing at 200°C for 1 h in air and subsequent pyrolysis at 800°C for 1 h in an Ar gas flow, porous SiOC beads were obtained. Freeze-dried beads showed lamellae-shaped macro-pore structures at a moderate freezing rate due to a phase separation behavior of PCS during freezing, while no lamellae pores were formed at a very high freezing rate. Water droplets formed in w/o emulsion converted to spherical pores after drying. The combined processes of producing PCS emulsion and freeze-drying of emulsion resulted in two types of macro-pores: lamellae-shaped and spherical pores. Meso-pores, of which specific surface area and average pore size were 71.5 m²·g⁻¹ and 4.85 nm, respectively, were formed in the SiOC strut.

Keywords: Porous SiOC bead, Freeze-drying, Polymer emulsion, Polycarbosilane

1. Introduction

Since the development of organosilicon polymers, ceramic processing via pyrolysis of polymer precursors has been received much attention because new applications and novel design of ceramic materials can easily be facilitated [1,2]. Various shapes of polymer-derived ceramics (PDCs), namely films, fibers, powders, porous media and other complexes, are obtained by manipulating polymer solutions.

Polymer-derived porous SiOC have been produced by several strategies such as foaming process [3], combination of template with foaming [4], replica technique [5], soft and hard templating [6-8] and emulsion processing [9,10]. A recent study on the PDCs from emulsions of polymeric precursor demonstrates that controllable sample sizes with versatile porosity are easily obtained [11]. Emulsion process has many advantages because it provides diverse droplet sizes and structures via phase separation and phase inversion [12,13].

We prepared porous PDCs by a combination of polymer emulsion and freeze-drying method. A w/o emulsion was prepared by mixing water and PCS dissolved *p*-xylene. By freeze-drying the emulsion and subsequent heat-treating, highly porous SiOC beads were obtained. It has been shown that the shape of a highly aligned pore channel is simply obtained by control the cooling rate during freezing of precursor solution [14]. Therefore, it is expected that pore structures are manipulated by freezing the solvent while maintaining the structures of droplets in w/o emulsion. The morphology of the porous SiOC beads was observed and pore-forming procedure was discussed.

2. Experimental

PCS as a starting material was purchased from ToBeMTEch. Its molecular weight is 60886 Da (Fig. S1, Electronic supplementary information, ESI), and weight loss up to 1000°C under Ar gas atmosphere is 20 wt.% (Fig. S2, ESI). It completely melts at 300°C (Fig. S3, ESI). We chose SXS (Stepanate SXS-93, Stepan) and *p*-xylene (anhydrous, 99%, Sigma-Aldrich) as an emulsifier and a solvent, respectively. The melting point of *p*-xylene is 13°C, which is highest among three types of xylene. In the freeze-drying procedure of PCS emulsions, 0.45~1.35 g of PCS and 0.5 g of SXS were dissolved in 3 mL of *p*-xylene under mild agitation for 24 h. To produce emulsion, 7~10 mL of de-ionized water was slowly added while vigorously stirring the solution using a magnetic bar. Then, the emulsion was added drop by drop using micro-pipet onto a liquid N₂ bath to form PCS beads, which normally showed 1~2 mm in size (Fig. S4, ESI). The beads were immediately put into a vacuum chamber and dried at 13.3 Pa for 24 h at room temperature. They were cured at 200°C for 1 h in air, and then heat-treated at 800°C at a ramp rate of 2°C/h for 1 h in an electric tube furnace under an Ar gas flow.

The pore structures of the freeze-dried and their heat-treated beads were observed by a field-emission scanning electron microscope (FE-SEM; Quanta 600 FEG, FEI). The atomic vibrations of the heat-treated beads were recorded by a Fourier transform infrared spectrometer (FT-IR; Nicolet 6700, Thermo Scientific) in transmission geometry. Carbonaceous state of heat-treated beads was characterized by Raman spectrometer (Witec Confocal Raman) at the wavelength of 514 nm. The specific surface area and pore size were analyzed by BET (Brunauer, Emmet and Teller) theory with N₂ adsorption (ASAP 2020, Micromeritics) at -196°C.

3. Results and discussion

Freeze-drying usually develops a unique pore structures due to the phase separation of the polymer solutions. Fig. 1 shows how the pore structures can be varied by introducing freeze-drying procedure. No pores are found in a mass from slowly dried PCS solution (Fig. 1a). On the contrary lamella-shaped pores are well developed in freeze-dried PCS (Fig. 1b). It is known that polymer membranes are manufactured using a thermally induced phase separation (TIPS) [15,16]. During the procedure, liquid-liquid phase separation into polymer-rich and polymer-poor phases occurs as the temperature of the solution decreases. Polymers exist as single crystals at a very low concentration while polymers form supramolecular architectures of lamellae at a high concentration [15]. Therefore lamellae structures shown in Fig. 1b can be explained by TIPS that occurs during freezing.

Fig. 2 shows the SEM images of freeze-dried PCS emulsion. Both lamellae pores and spherical voids are found in the as-dried sample (Fig. 2a). Lamellae pores are the same shapes as in Fig. 1b, and they are formed during freezing of PCS dissolved *p*-xylene solution. Large spherical voids are the traces of water droplets in PCS emulsion. Therefore there exist two types of pores in the freeze-dried PCS emulsion; lamellae and spherical shaped pores. Surface of a bead is shown in Fig. 2b. Lamella structures are not seen on the surface and pore inlets are rounded. When emulsion droplets contacted with the liquid N₂, droplets were kept hovering on liquid N₂ due to the Leidenfrost effect for about 10 s before sinking into liquid N₂ bath. Sufficient time is provided for PCSs to be melt partially on the surface by the heat of evaporation. This results in rounding pore inlets and blocking thin lamellae pores. Fig. 2c and Fig. 2d show the SEM images of freeze-dried beads after pyrolysis at 800°C for 1 h under an Ar gas flow. Lamellae structures composed of many thin slabs are quite obvious in Fig. 2d

where the image was taken at the right angle of Fig. 2c. FT-IR analysis of heat-treated beads (Fig. S5, ESI) revealed several absorption peaks; Si-O stretching (1070 cm^{-1}), O-Si-O bending (785 cm^{-1}), Si-C stretching (878 cm^{-1}), Si-C vibration (613 cm^{-1}), and graphitic carbon vibration (around 1440 cm^{-1}). Therefore, we can identify that the heat-treated beads have Si-O bonds as well as Si-C bonds. It is thought that oxygen atoms were incorporated either from SXS or during curing process in air.

The development of the lamella structure is related with the thermal gradient in TIPS. We see that lamellae structures are randomly distributed as shown in Fig. 1 and Fig. 2. That is because the whole surfaces of emulsion droplets contact with liquid N_2 during freezing. The quenching rate was varied to examine the effect of thermal gradient on the lamella shaped structure. First, PCS emulsion was put on 2 mm thick graphite substrate, and it was forced to quick immersion into liquid N_2 bath. The freezing time was much shorter than typical 10 s of bead formation, so there was not enough time for developing lamella shaped structure (Fig. 3a) which resulted in spherical pores only. Second, when emulsion-covered graphite substrate was being touched on the surface of liquid N_2 bath in order to decrease the temperature of the substrate slowly (non-direct contact between emulsion and liquid nitrogen), well-aligned lamellae-shaped structures were developed as shown in Fig. 3b. This suggests that the degree of lamella structure development can be controlled by varying cooling process.

It is worth while to mention on the characteristics of pores that are formed inside the SiOC strut. It is known that PDCs derived from PCS produce free carbon phase which affects on the properties like BET surface area and pore size of PDCs [17]. Free carbons are usually incorporated into PDCs from polymer and eventually act as an inhibitor to crystallization of PCS during pyrolysis [17,18]. Raman spectrum of porous bead heat-treated at 800°C for 1 h in an Ar gas flow (Fig. S6, ESI) shows the D-band (disordered carbon state) at 1335 cm^{-1} , G-

band (reflecting the bond stretching of sp^2 carbon) at 1560 cm^{-1} , and broad 2D vibration at around 2670 cm^{-1} . The peaks are broad and the intensity of the D-band is stronger than that of the G-band, which proves the disordered nature of segregated carbon atoms.

The nature of porosity generated inside the SiOC strut was subsequently investigated by N_2 gas adsorption-desorption (Fig. S7, ESI). The isotherm for the sample shows a clear and wide hysteresis loop at $P/P_0 = 0.45$ to 0.99 , which is a typical isotherm of Type IV with ink-bottle type meso-pores [19]. The analysis revealed $71.5\text{ m}^2\cdot\text{g}^{-1}$ of BET surface area, $0.060\text{ cm}^3\cdot\text{g}^{-1}$ of total pore volume, $0.045\text{ cm}^3\text{ g}^{-1}$ of meso-pore volume, and $0.0048\text{ cm}^3\cdot\text{g}^{-1}$ of micro-pore volume. This suggests that meso-pores occupy about 75% of total pore volume. The pore size distribution obtained by BJH adsorption method of the N_2 adsorption isotherm indicated a meso-pore peak at 2.7 nm of pore diameter and a heterogeneous meso-pore size distribution (inset in Fig S7). The average pore size was 4.85 nm.

4. Conclusions

In summary, porous SiOC beads were prepared by freeze-drying PCS emulsions. Freeze-drying led to lamellae-shaped pores while slow drying didn't form any type of macro-pores. Water droplets in w/o emulsion were changed into spherical pores under freeze-drying. Therefore two types of pores, lamella-shaped and spherical pores, were obtained by freeze-drying w/o emulsion. The direction of lamella-shaped pores was aligned along temperature gradient direction. Gas adsorption analysis showed that meso-pores were formed inside the SiOC strut.

Acknowledgment This study was partially supported by Seoul National University of Science and Technology. The authors thank N. Wannemacher for assistance with the BET analysis.

References

- [1] Colombo P, Mera G, Riedel R, Sorarù GD. *J Am Ceram Soc* 2010;93:1805-37.
- [2] Mera G, Navrotsky A, Sen S, Kleebe H-J, Riedel R. *J Mater Chem A* 2013;1:3826-36.
- [3] Zeschky J, Höfner T, Arnold C, Weißmann R, Bahloul-Hourlier D, Scheffler M, Greil P. *Acta Materialia* 2005;53:927–37.
- [4] Vakifahmetoglu C, Colombo P, Pauletti A, Martin CF, Babonneau F. *Int J Appl Ceram Technol* 2010;7:528–35.
- [5] White RA, White EW, Weber JN. *Science* 1972;176:922-4.
- [6] Wang C, Wang J, Park CB, Kim YW. *J Ceram Proc Res* 2009;10:238-42.
- [7] Shibuya M, Takahashi T, Koyama K. *Compos Sci Technol* 2007;67:119–24.
- [8] Biasetto L, Francis A, Palade P, Principi G, Colombo P. *J Mater Sci* 2008;43:4119–26.
- [9] Bakumov V, Schwarz M, Kroke E. *J Eur Ceram Soc* 2009;29:2857–65.
- [10] Frind R, Oschartz M, Kaskel S. *J Mater Chem* 2011;21:11936-40.
- [11] Vakifahmetoglu C, Balliana M, Colombo P. *J Eur Ceram Soc* 2011;31:1481–90.

- [12] Mason TG, Wilking JN, Meleson K, Chang CB, Graves SM. *J Phys-Condensed Mat* 2006;18:R635-66.
- [13] Sajjadi S, Zerfa M, Brooks BW. *Colloid Surf A* 2003;218:241-54.
- [14] Yoon BH, Lee EJ, Kim HE, Koh YH. *J Am Ceram Soc* 2007;90:1753-9.
- [15] van de Witte P, Dijkstra PJ, van den Berg JWA, Feijen J. *J Membrane Sci* 1996;117:1-31.
- [16] Gao CY, Li A, Feng LX, Yi XS, Shen JC. *Polym Int* 2000;49:323-8.
- [17] Williams HM, Dawson EA, Barnes PA, Rand B, Brydson RMD, Brough AR, *J Mater Chem* 2002;12:3754-60.
- [18] Sorarù GD, Pederiva L, Latournerie J, Raj R. *J Am Ceram Soc* 2002;85:2181-7.
- [19] Kitagawa S, Kitaura R, Noro S. *Angew Chem Int Ed* 2004;43: 2334-75.

Figure captions

Fig. 1. (a) SEM images of slowly dried and (b) freeze dried PCS solution. The loading of PCS in *p*-xylene was 0.15 g/mL for both samples. Samples were heat-treated at 800°C for 1 h in an Ar gas flow. The length of the scale bar is 50 μm.

Fig. 2. SEM images of porous beads from freeze drying of PCS emulsions. (a) Fracture surface of as freeze dried sample. (b) Outer surface of as freeze dried bead. (c,d) Fracture surfaces of beads heat-treated at 800°C for 1 h in an Ar gas flow. The loading of PCS and SXS in *p*-xylene was 0.45 g/mL and 0.17 g/mL, respectively. The volume ratio of *p*-xylene to water was 3:10. The length of the scale bar is 100 μm.

Fig. 3. SEM images showing different microstructures due to the degree of undercooling. (a) Fracture surface of bead undergone high degree of undercooling, and (b) low degree of undercooling. The temperature gradient was set along the horizontal direction. The length of the scale bar is 40 μm.

Fig. S1. GPC analysis to measure the molecular weight of PCS.

Fig. S2. TG analysis of PCS.

Fig. S3. Photographs showing melting of PCS.

Fig. S4. Digital photo showing freeze-dried beads.

Fig. S5. FT-IR spectrum of SiOC beads heat-treated at 800°C for 1 h in an Ar gas flow.

Fig. S6. Raman spectrum of beads heat-treated at 800°C for 1 h in an Ar gas flow.

Fig. S7. N₂ gas adsorption-desorption isotherm of beads heat-treated at 800°C for 1 h in an Ar gas flow. The inset in the lower right corner shows the pore size distribution. S_{BET} , V_{total} , V_{meso} , V_{micro} , and D_{average} denote BET surface area, total pore volume, mesopore volume, micropore volume, and average pore size, respectively.

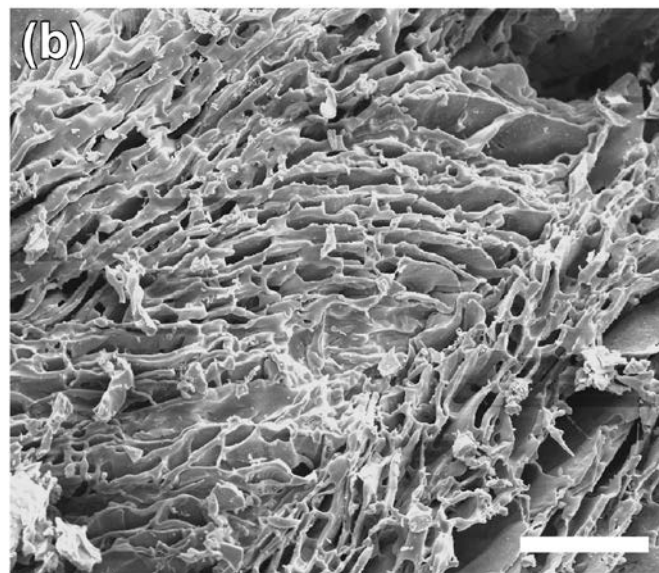
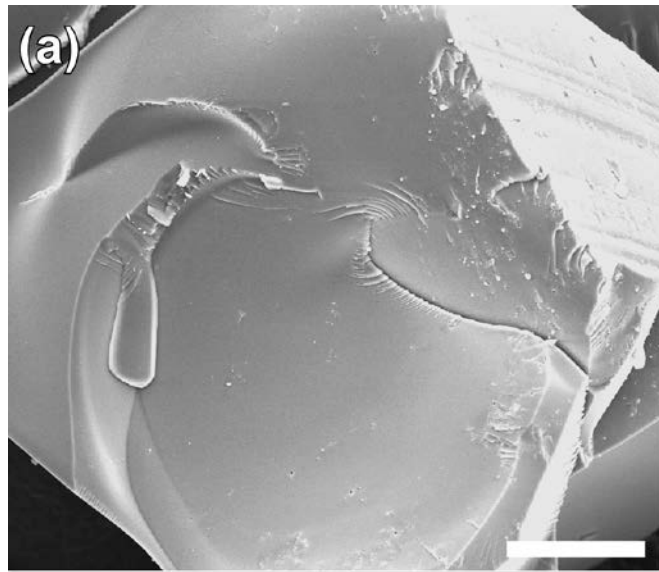


Fig. 1. Y. Hwang et al.

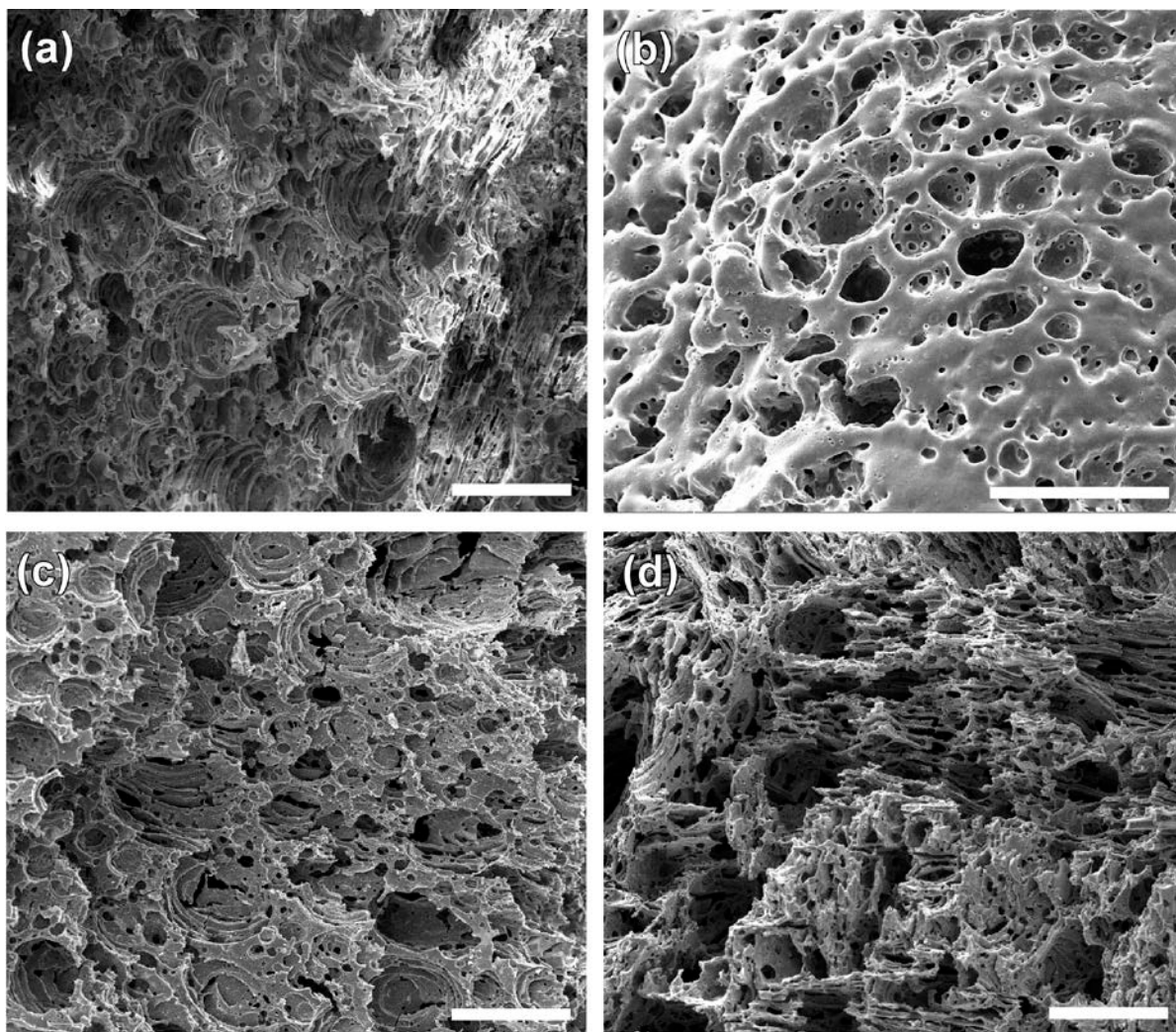


Fig. 2. Y. Hwang et al.

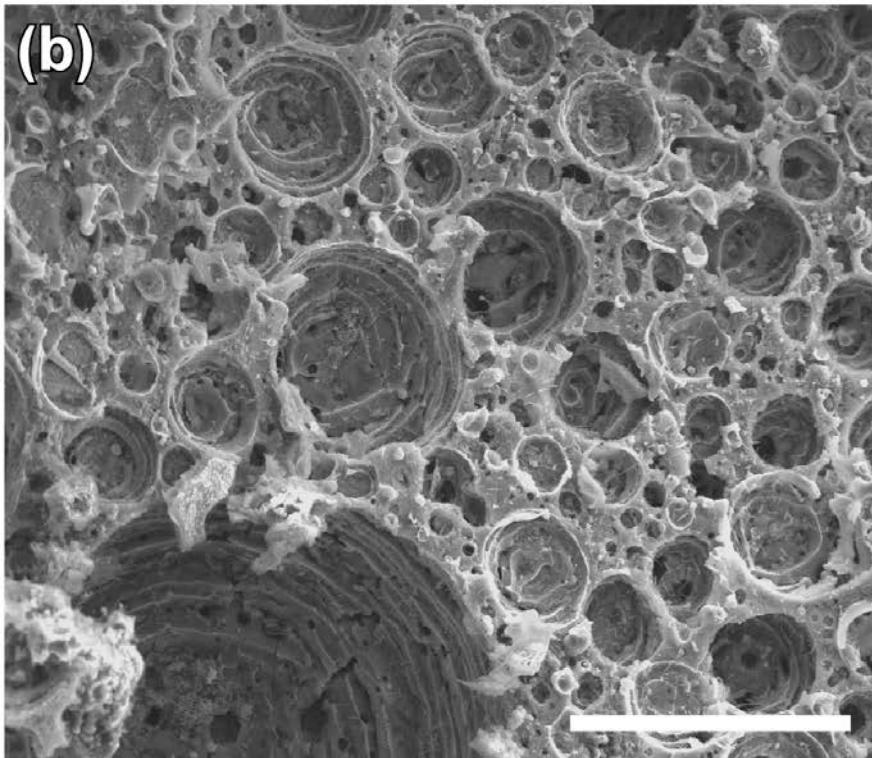
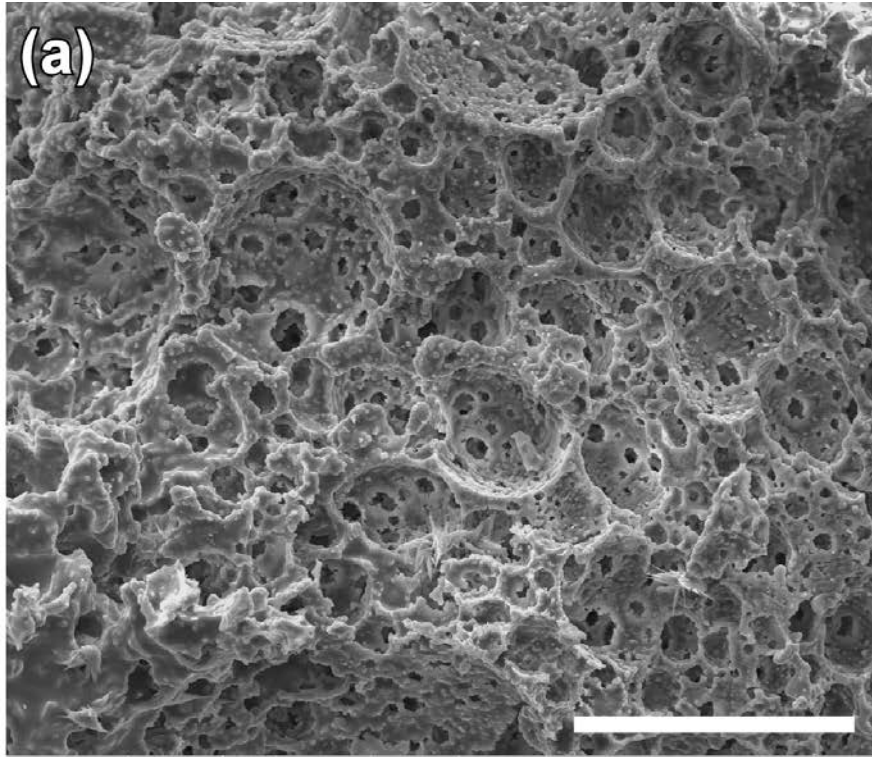
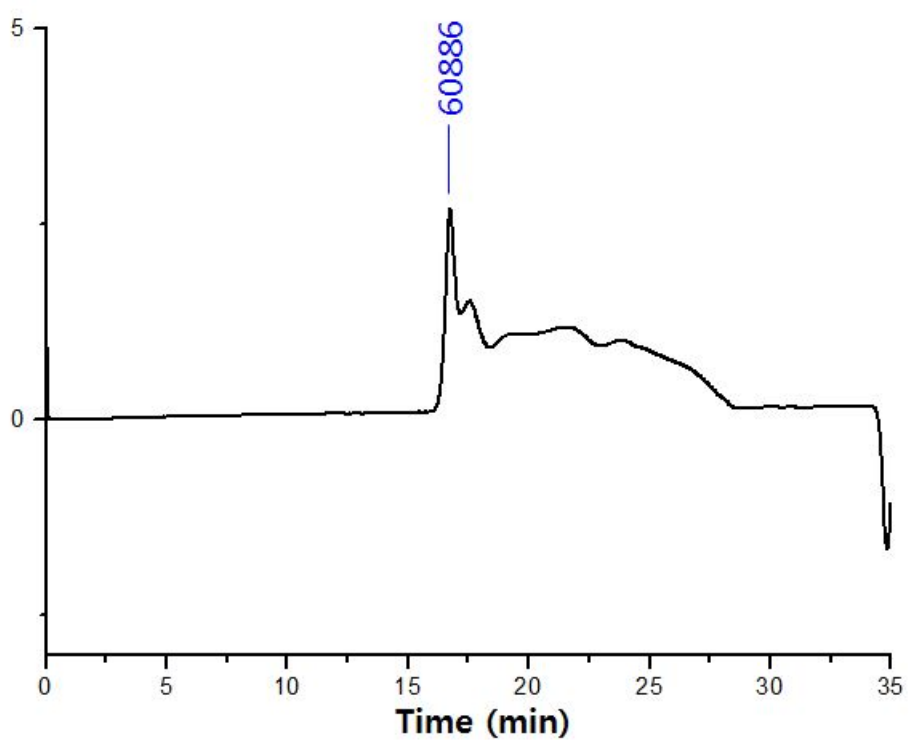


Fig. 3. Y. Hwang et al.



Broad Unknown Relative Peak Table

	Distribution Name	Mn (Daltons)	Mw (Daltons)	MP (Daltons)	Mz (Daltons)	Mz+1 (Daltons)	Polydispersity	Mz/Mw	Mz+1/Mw
1		1683	15044	60886	43495	56133	8.937670	2.891201	3.731224

Fig. S1. Y. Hwang et al.

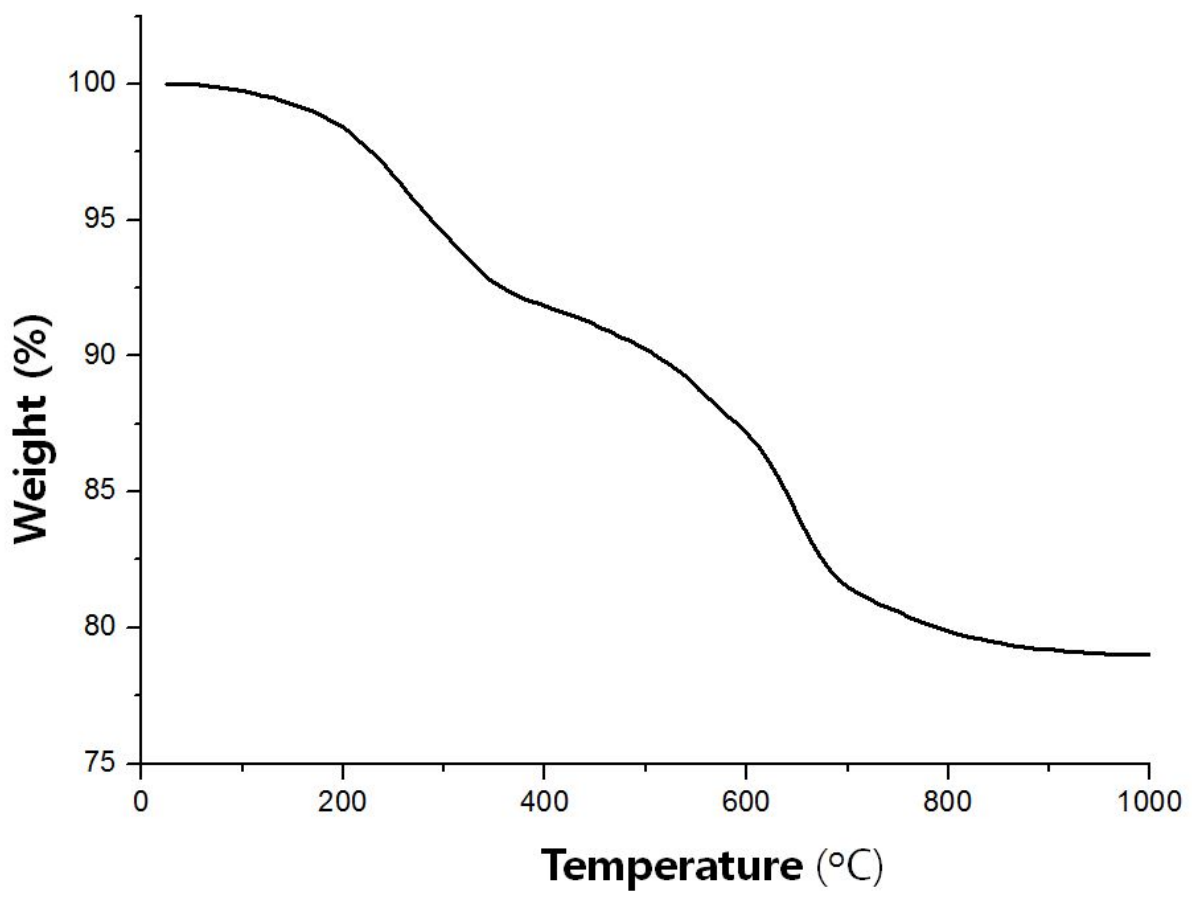


Fig. S2. Y. Hwang et al.



[140 °C]



[250 °C]



[300 °C]

Fig. S3. Y. Hwang et al.

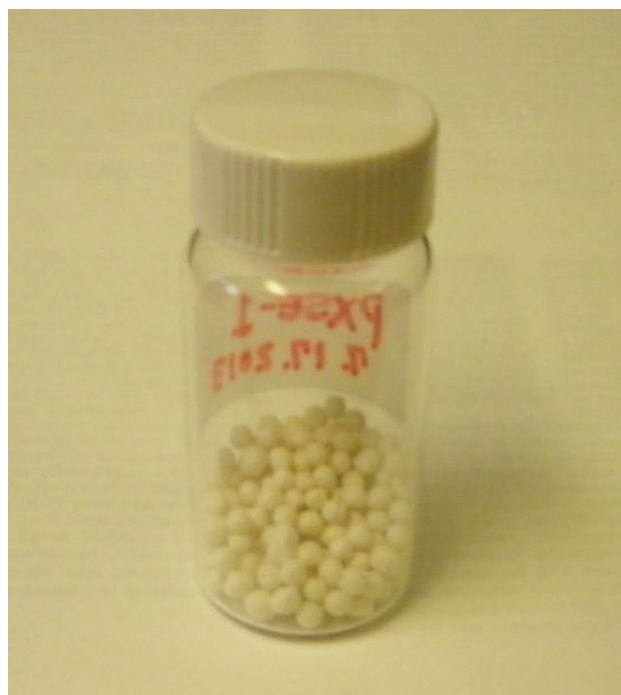


Fig. S4. Y. Hwang et al.

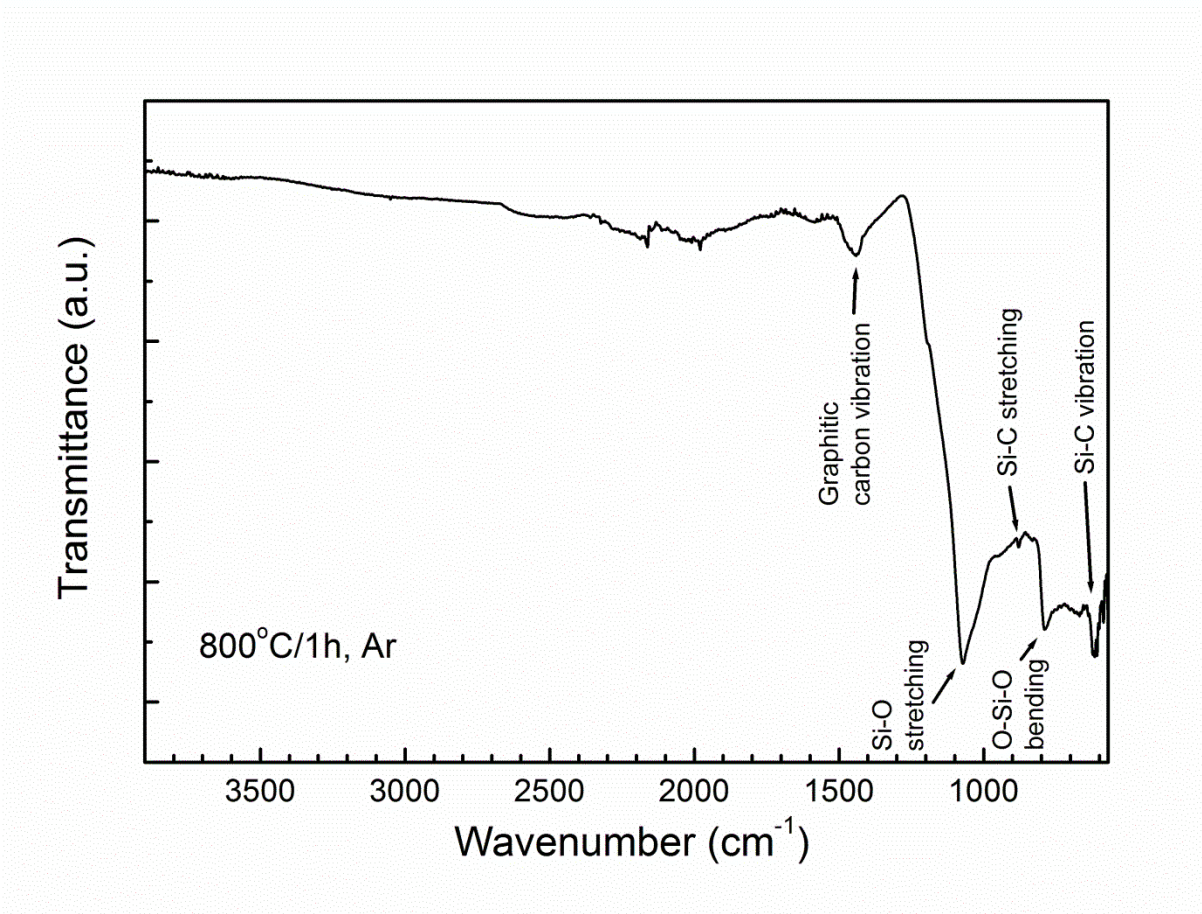


Fig. S5. Y. Hwang et al.

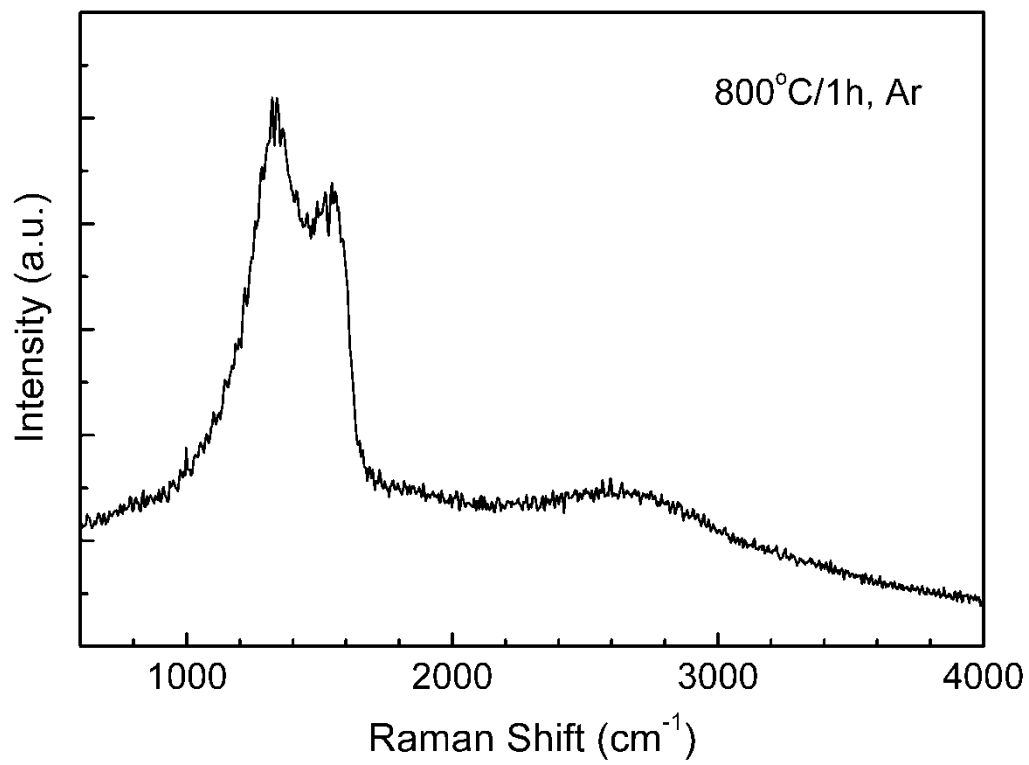


Fig. S6. Y. Hwang et al.

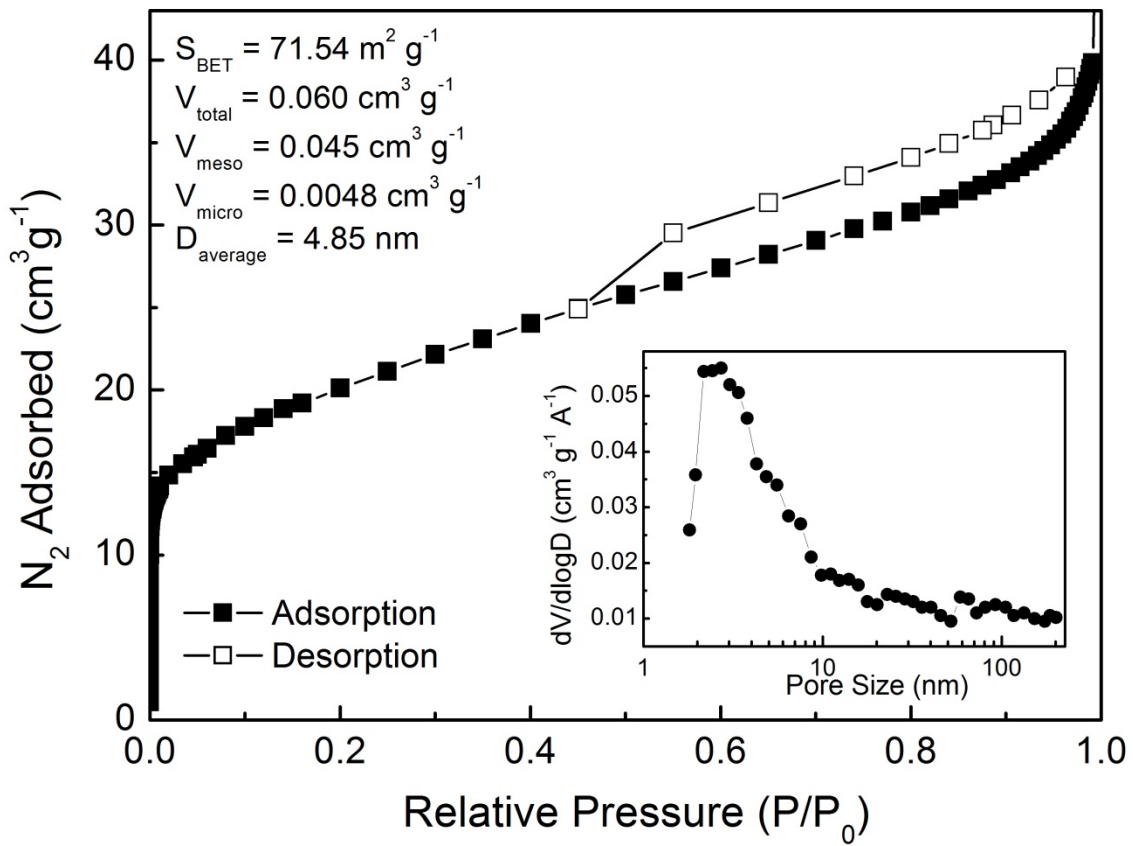


Fig. S7. Y. Hwang et al.